Acta Mech
https://doi.org/10.1007/s00707-019-02464-1

ORIGINAL PAPER

Shilei Zuo · Yang Liu · Kai Zhang · Gengkai Hu

Wave boundary control method for vibration suppression of large net structures

Received: 6 March 2019 / Revised: 6 May 2019

Abstract Large net structures used in engineering can easily get into vibration under external excitations; however, the corresponding vibration control strategy still remains challenging. In this paper, a wave boundary control (WBC) strategy is proposed for the vibration suppression of large net structures. The stability of the controlled structures is confirmed by using inverse Fourier transform, transfer function analysis, and numerical simulation. When WBC controllers are set at all boundaries and excitations come from the boundaries, dynamic responses for all the strings of the net structures can quickly reduce to zero without any residual vibration. The effects of different observations, controls, and distributions of sensors on the control laws are discussed. As an application, a method for reducing the number of controllers for large net structures is finally proposed. The research provides theoretical guidance for vibration control of large net structures.

1 Introduction

Large net structures are widely used in various engineering fields due to their excellent characteristics, including light weight, small stowed volume, and high stiffness when stretched [1–3]. However large net structures can easily start to vibrate under external excitations. For example, in space, alternating thermal loads, the impact of space debris, and adjustments of the spacecraft's attitude can cause out-of-plane vibration of a net structure. The structural vibration will affect the normal operation and even damage the structure. Accordingly, it is necessary to investigate vibration control strategies for large net structures [4,5].

The vibration control strategies for structures usually can be divided into active control and passive control. Compared with passive control, active vibration control has strong flexibility and reliability and can avoid several deficiencies [6,7]. As one of the widely used active control methods, modal control based on the modal theory requires truncation of finite modes [8,9]. However, the truncation of finite modes is inaccurate for large net structures owing to the dense structural modes. As a result, modal control is only effective for truncated models, leading to modal spillovers [8,10]. On the other hand, for large net structures, shocks or disturbances do not immediately make the whole structure vibrate, but propagate gradually from the disturbance pointed to the whole structure in the form of elastic waves. Consequently, the modal control is only effective for small net structures. Therefore, several researcher have begun to study the vibration control of structures based on wave theory. In 1984, Mace [11] studied the wave characteristics of a beam and pointed out that the reflection and transmission of an elastic wave can be determined by reflection and transmission coefficients when the elastic wave passes through a discontinuity. On the basis of the previous wave characteristic study, Mace [12] eliminated the transmission wave by adjusting the transmission matrix and realized the active isolating control of the vibration at the control point downstream on the beam. In the same period, wave control for spacecraft structures was investigated by Von Flotow [13]. In his study, the active control of these structures was

S. Zuo · Y. Liu · K. Zhang (✉) · G. Hu
School of Aerospace Engineering, Beijing Institute of Technology, Beijing 100081, China
E-mail: zhangkai@bit.edu.cn

Published online: 15 July 2019

approached from the point of view of actively modifying the natural disturbance propagation paths. After that, Tanaka [14,15] proposed a wave-based active sinking method for beam structures. Ruzzene [16] employed periodic arrays of shunted, piezoelectric patches to control vibrations and waves propagating over the surface of plate structures. Wu and Li [17] investigated the vibration band gaps of a square lattice structure based on wave theory. Watanabe et al. [18] studied the vibration suppression on transverse vibration of flexible space tether systems by a wave-absorbing control method. Since the controllers are designed directly based on wave equations in the full frequency domain, the wave-based methods have shown the ability to avoid modal spillover and modal truncation compared to the traditional modal control methods [19,20]. However, most of the wave controls are aimed at one-dimensional structures, since the wave equation of one-dimensional structures is easy to solve.

From a mathematical point of view a large net structure is often considered as an original distributed parameter system because the motion of such a system is described by variables depending on both time and space [21]. For the control of the distributed parameter system, boundary control, where actuators are applied only on the structural boundary, is more economical and effective. Some researchers have also done research on the boundary control. William's study showed that the boundaries can be actively controlled to establish and maintain standing waves [22]. In addition, the boundary actuator was located at one end of the beam-like mass–spring arrays while absorbing the vibration by canceling the outgoing waves [23]. Kreuzer and Steidl presented a method for controlling the torsional vibrations and stick-slip vibrations by exactly decomposing the drill string dynamics into two traveling waves traveling in the directions of the top drive and the drill bit [24]. Hossein Kaviani et al. [25] investigated the vibration of a flexible satellite with flexible appendages and designed the control torque and forces based on the boundary control method. Krstic [26] introduced the backstepping method into the partial differential equation and developed the boundary control method. Then, Wang et al. [27,28] designed the output feedback controller via the backstepping method to suppress the vibration in the cable elevator. Zhao et al. [29,30] proposed a basic boundary control scheme to suppress the string's vibration based on the backstepping method. Then, he applied the boundary control strategy to flexible riser systems [31,32] and axially moving systems [33]. In the authors' previous work [34], a collocated control strategy was proposed. The wave-absorbing control strategy took the negative transverse velocity at the end of the string as the feedback signal of the control law ($u(t) = -K w_t(t, 1)$). Compared with the collocated control strategy [34], non-collocated systems are more difficult to control due to stability concerns [35]. Unfortunately, for two-dimensional large net structures, the work used the wave-based non-collocated boundary control method which is still little reported on. Thus, in this paper, a wave boundary control (WBC) method is proposed to investigate the vibration control of net structures. In Sect. 2, the wave boundary control method is introduced and the stability of net structures is analyzed. The inverse Fourier transform is applied to explore the principle of stability. The physical mechanism is that poles of the net structure in the frequency domain are eliminated by using our proposed WBC method, and further structural vibration (standing wave) is tailored into traveling waves. In Sect. 3, the control laws corresponding to different observations and different distributions of the sensors are derived and summarized. In Sect. 4, as an application, weaving design boundaries for reducing the number of controllers for large net structures is proposed and numerical simulations are carried out to prove the effectiveness of the wave boundary control strategy. These are the latest research results which have not been reported in the previous paper [34].

2 Wave boundary control method and stability analysis

2.1 Single string

In this study, the tensions of any continuous strings are approximately constant because displacement responses of the net structures are quite small [36]. Thus, a linear analysis can be permitted [37]. Such a linear system has a negligible Young's modulus and cannot transmit longitudinal waves along its length [38]. As a result, only the transverse displacement is considered for each string. Besides, both gravity and damping are ignored [39].

The proposed WBC method is established based on the one-dimensional linear wave equation. The free vibration of a single string model is described by

$$T\frac{\partial^2 u}{\partial x^2} - \rho\frac{\partial^2 u}{\partial t^2} = 0, \tag{1}$$

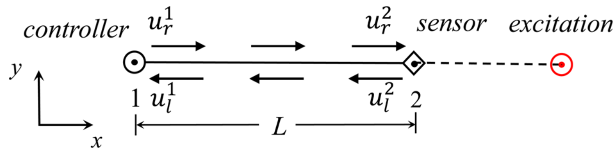

Fig. 1 Boundary control scheme for a single string. The controller and sensor are applied at left and right, respectively, while the excitation is at the far end of the right

where $u(x, t)$ is the transverse displacement of the string; T and ρ are the pretension and mass per unit length, respectively; x and t are the space coordinate along the string and time, respectively.

The general solution of Eq. (1) can be considered as a sum of a leftward and a rightward traveling wave mode [38,40] in the frequency domain:

$$u(x, \omega) = w_l(\omega)\, e^{ikx} + w_r(\omega) e^{-ikx} = u_l(x, \omega) + u_r(x, \omega), \tag{2}$$

where ω is the angular frequency and $i = \sqrt{-1}$. k is the wave number and given by $k = \omega/c = \sqrt{\rho\omega^2/T}$, $c = \sqrt{T/\rho}$ is the wave speed. $u_l(x, \omega)$ and $u_r(x, \omega)$ are the waves traveling toward the left and right along the string, respectively.

As shown in Fig. 1, the initial conditions of the string (both the net structures in the following) are $u\,|_{t=0}(x) = \frac{\partial u}{\partial t}\,|_{t=0}(x) = \frac{\partial^2 u}{\partial t^2}\,|_{t=0}(x) = 0$. The displacement for an actuator and a sensor expressed as U_c and U_s, respectively, are also considered to be the superposition of two directional traveling waves:

$$\begin{cases} U_c = u_l^1 + u_r^1, \\ U_s = u_l^2 + u_r^2, \end{cases} \tag{3}$$

where u_l^1, u_l^2, u_r^1, and u_r^2 are the traveling wave components of the related boundaries.

According to the traveling wave continuity condition, the four wave components in the string with length L have the following relationship:

$$\begin{cases} u_l^1 = u_l^2 \cdot e^{-ikL}, \\ u_r^1 = u_r^2 \cdot e^{ikL}, \end{cases} \tag{4}$$

where the delay time e^{-ikL} between the wave components is related to the distance L between the two points and the wave number k toward the same direction.

The main idea of the WBC method is that the actuator reduces the system energy by reducing a certain reflected traveling wave to zero. Therefore, it can be written as

$$u_r^1 = 0. \tag{5}$$

Substituting Eqs. (4) and (5) into Eq. (3), one can obtain the expression of the control law as follows:

$$U_c = e^{-ikL} \cdot U_s. \tag{6}$$

Therefore, the standing waves will not form in the whole string and the vibration of the structure is therefore suppressed. The derivation process above is based on displacement control. When the actuator applies a force control, which is expressed as F_c, one can obtain the solution by the same derivation process.

$$F_c = -ikT \cdot e^{-ikL} \cdot U_s. \tag{7}$$

2.2 Orthogonal cross-string structures

Figure 2a shows an orthogonal cross-string structure which is constituted by four single strings and knotted vertically at point O. An excitation is applied at point A and a controller is set at point C, while the boundary points B and D are fixed. In the WBC method, displacement continuity condition and force coordination are required. Namely, the displacements of different strings at a certain intersection must be identical and the transverse force of the junction caused by the pretension of the connected strings should be balanced.

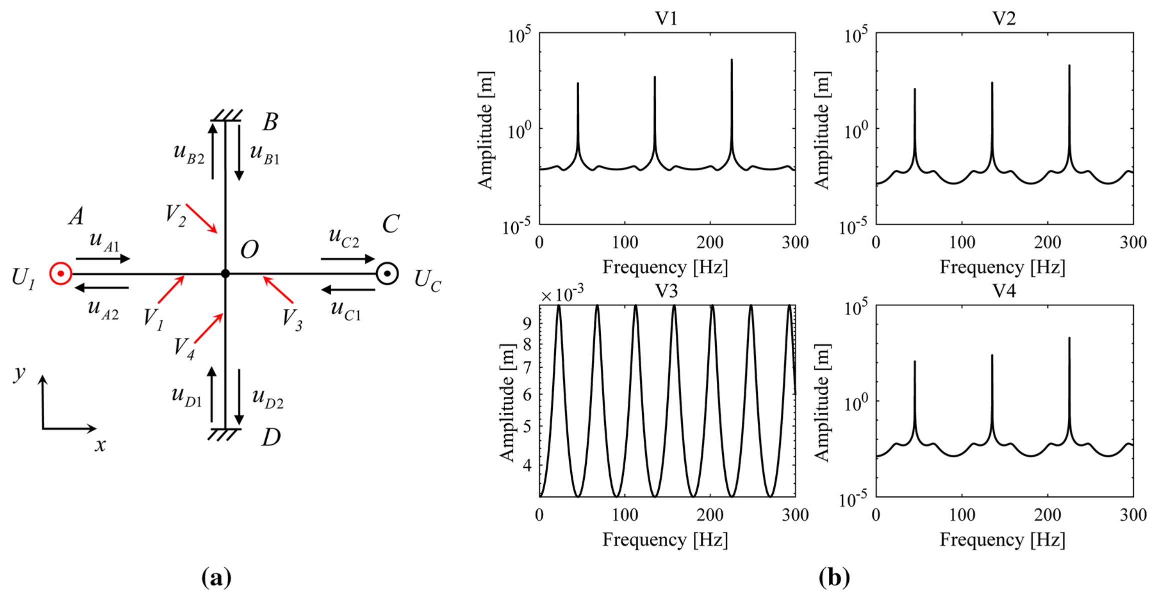

Fig. 2 Orthogonal cross-string structure and the corresponding frequency-domain responses. **a** The length of each string is L. U_1 is the excitation along out-of-plane. u_{A1}, u_{A2}, u_{B1}, u_{B2}, u_{C1}, u_{C2}, u_{D1}, and u_{D2} are the traveling wave components of the corresponding boundaries, respectively. An excitation is applied at the boundary point A, and one controller is set at point C. V_1, V_2, V_3, and V_4 mean the frequency-domain responses corresponding to string AO, BO, CO, DO whose distance from the point O is $3L/5$. **b** Frequency responses of the orthogonal cross-string structure with one controller

To get the control law of the orthogonal cross-string structure, the model in Fig. 2a is considered. The boundary conditions are

$$\begin{cases} u_{A1} + u_{A2} = U_1, \\ u_{B1} + u_{B2} = 0, \\ u_{C1} + u_{C2} = U_C, \\ u_{D1} + u_{D2} = 0, \end{cases} \tag{8}$$

where u_{A1}, u_{A2}, u_{B1}, u_{B2}, u_{C1}, u_{C2}, u_{D1}, and u_{D2} are the traveling wave components of the corresponding boundaries, respectively.

The displacement continuity conditions at junction O are as follows:

$$\begin{cases} u_{A1} \cdot G^{-1} + u_{A2} \cdot G = u_{B1} \cdot G^{-1} + u_{B2} \cdot G, \\ u_{B1} \cdot G^{-1} + u_{B2} \cdot G = u_{C1} \cdot G^{-1} + u_{C2} \cdot G, \\ u_{C1} \cdot G^{-1} + u_{C2} \cdot G = u_{D1} \cdot G^{-1} + u_{D2} \cdot G, \end{cases} \tag{9}$$

where $G = \mathrm{e}^{ikL}$.

The force equilibrium equation at junction O is

$$(u_{A1} + u_{B1} + u_{C1} + u_{D1}) \cdot G^{-1} \cdot ikT + (u_{A2} + u_{B2} + u_{C2} + u_{D1}) \cdot G \cdot (-ikT) = 0. \tag{10}$$

By solving Eqs. (8), (9), and (10) together, the traveling waves on each string can be obtained as

$$\begin{cases} u_{A1} = \frac{G^2(2G^2U_1+U_1-U_C)}{2(G^4-1)}, \quad u_{A2} = \frac{(U_C-U_1)G^2-2U_1}{2(G^4-1)}, \\ u_{B1} = u_{D1} = -\frac{G^2(U_1+U_C)}{2(G^4-1)}, \\ u_{B2} = u_{D2} = \frac{G^2(U_1+U_C)}{2(G^4-1)}, \\ u_{C1} = \frac{G^2(2G^2U_1-U_1+U_C)}{2(G^4-1)}, \quad u_{C2} = \frac{(U_1-U_C)G^2-2U_C}{2(G^4-1)}. \end{cases} \tag{11}$$

The reflected wave of the controlled boundary (see point C) is zero, namely $u_C^1 = 0$:

$$\frac{G^2\left(2G^2 U_c - U_1 + U_C\right)}{2\left(G^4 - 1\right)} = 0. \tag{12}$$

Thus, one can get the control law

$$U_C(x, \omega) = \frac{U_1}{2G^2 + 1}. \tag{13}$$

Substituting Eq. (13) into Eq. (8), and resolving Eqs. (8)–(10) (or simply substituting Eq. (13) in Eq. (11)), one can obtain the traveling waves in the structure

$$\begin{cases} u_{A1} = \frac{2G^4 U_1}{(G^2-1)(2G^2+1)}, \quad u_{A2} = -\frac{(G^2+1)U_1}{(G^2-1)(2G^2+1)}, \\ u_{B1} = u_{D1} = -\frac{G^2 U_1}{(G^2-1)(2G^2+1)}, \\ u_{B2} = u_{D2} = \frac{G^2 U_1}{(G^2-1)(2G^2+1)}, \\ u_{C1} = 0, \quad u_{C2} = \frac{U_1}{2G^2+1}. \end{cases} \tag{14}$$

The displacement of an arbitrary point on a string in its local coordinate system can be expressed as

$$V_m(x, \omega) = u_{j1} \cdot \mathrm{e}^{-ikx} + u_{j2} \cdot \mathrm{e}^{ikx}, \quad (j = A, B, C, D)\ (m = 1, 2, 3, 4). \tag{15}$$

Then, we get

$$V_1(x, \omega) = \frac{\mathrm{e}^{-ikx}(2G^4 - \mathrm{e}^{2ikx}(G^2 + 1))G^{-2}U_1}{3G^2}\left(\frac{1}{G^2 - 1} - \frac{1}{2G^2 + 1}\right), \tag{16}$$

$$V_2(x, \omega) = V_4(x, \omega) = \frac{(\mathrm{e}^{ikx} - \mathrm{e}^{-ikx})U_1}{3}\left(\frac{1}{G^2 - 1} - \frac{1}{2G^2 + 1}\right), \tag{17}$$

$$V_3(x, \omega) = \frac{\mathrm{e}^{ikx} U_1}{2G^2 + 1}. \tag{18}$$

Figure 2b shows the frequency responses corresponding to the orthogonal cross-string structure (Fig. 2a). The peak value in the diagram represents the vibration of the string. The responses of V_1, V_2, and V_4 are about five orders of magnitude larger than that of V_3 (the peak value in V_1 is 3914 and the value in V_3 is 0.0099 whose ratio is about 4×10^5). Namely, the string OC is controlled but vibration still exists in string OA, OB, and OD.

The series expansion methods can be used to investigate the vibrations [41]. In this paper, in order to explore the principle of stability, the inverse Fourier transform (IFT) is applied to transform the frequency-domain response V_3 into the time domain by using Taylor's formula $\frac{1}{1-x} = \sum_n^\infty x^n, \forall x : |x| < 1$:

$$\frac{1}{2G^2 + 1} = -\frac{G^{-2}}{2} \cdot \frac{1}{1 - (-\frac{1}{2}G^{-2})} = -\frac{G^{-2}}{2}\sum_0^\infty \left(-\frac{1}{2}\right)^n G^{-2n}. \tag{19}$$

Then, the inverse Fourier transform of Eq. (18), that is the response in the time domain, can be expressed as

$$V_3\,(x, t) = \sum_{n=0}^\infty \frac{(-1)^n}{2^{n+1}} U_1\left(t - 2\,(n + 1)\,\frac{l}{c} + \frac{x}{c}\right), \tag{20}$$

where the U_1 is an external excitation and the $\left(t - 2\,(n+1)\,\frac{l}{c} + \frac{x}{c}\right)$ is the variation of U_1.

Because one controller is set at point C, traveling waves have attenuated amplitudes $(1/2)^n$. Because the series Eqs. (19) and (20) are convergent, the response V_3 eventually tends to be convergent which indicates that the string OC will be stable when a controller is applied at point C. The time-domain response (20) also tends to be convergent as the time t and series n tend to be infinity. Therefore, Eq. (19) can be regarded as an attenuation term. However, in Eqs. (16) and (17), the term $1/(G^2 - 1)$ cannot be expressed as the terms of Taylor expansion. Since $G = \pm 1$ are the poles, the term $1/(G^2 - 1)$ can be regarded as a residual term. The

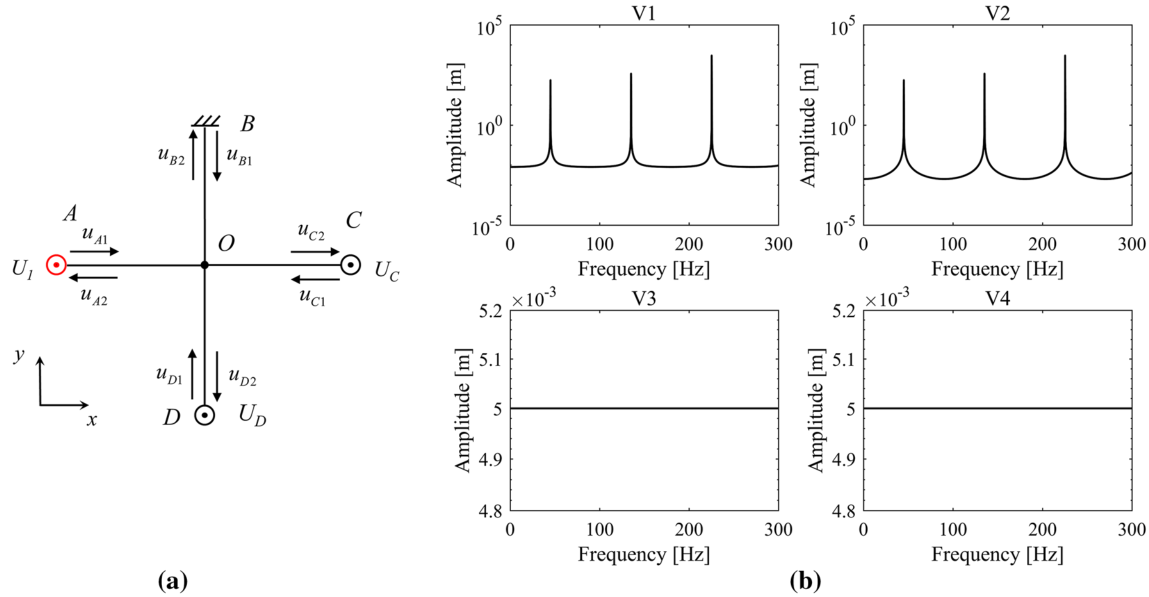

Fig. 3 Orthogonal cross-string structure with two controllers. **a** An out-of-plane excitation is at point A. Controllers are set at boundary points C and D. **b** The frequency response curves

residual term will not tend to be convergent when the time t is infinity, resulting in the residual vibration in the string. The whole structure in Fig. 2a shows instability when the controller is only set at boundary point C.

We further increase the number of controllers. As Fig. 3 depicts, a new controller is set at point D instead of the fixed boundary in Fig. 2a. According to the displacement continuity condition and force coordination with the same derivation, the wave boundary control laws and the frequency response expressions can be obtained (see (A.1)–(A.3) in the Appendix). Figure 3b shows the frequency responses corresponding to the orthogonal cross-string structure with two controllers at the boundaries. The vibrations still exist in strings OA and OB, while both strings OC and OD will be stable finally. The frequency response expressions (see (A.3) in the Appendix) are consistent with the previous conclusion that the string will produce the residual vibration when the item $1/(1 \pm G^m)$ exists. The item $1/(2G^2)$ in V_3 and V_4 (see (A.3) and (A.4) in the Appendix) is the time delay. The waves in strings OC and OD are gradually eliminated by the controllers.

In Fig. 4a, three controllers are set at boundaries. Applying the above derivation process, the frequency responses for Fig. 4a are given below:

$$\begin{cases} V_1(x,\omega) = \frac{(\mathrm{e}^{ikx} - 2\mathrm{e}^{-ikx} G^2) U_1}{1-2G^2}, \quad V_2(x,\omega) = -\frac{\mathrm{e}^{ikx} U_1}{1-2G^2}, \\ V_3(x,\omega) = -\frac{\mathrm{e}^{ikx} U_1}{1-2G^2}, \quad V_4(x,\omega) = -\frac{\mathrm{e}^{ikx} U_1}{1-2G^2}. \end{cases} \tag{21}$$

When four controllers are set at all boundary points and there is a small out-of-plane force excitation f_1 at the midpoint of the string AO, as shown in Fig. 4b, all of the reflected waves on the boundary are zero:

$$u_{A1} = 0, \quad u_{B1} = 0, \quad u_{C1} = 0, \quad u_{D1} = 0. \tag{22}$$

The control laws can be obtained as

$$U_A = \frac{i \cdot f_1 (2G - 1)}{4G^{3/2} \cdot k \cdot T}, \quad U_B = U_C = U_D = \frac{i \cdot f_1}{4G^{3/2} \cdot k \cdot T}. \tag{23}$$

The displacement response of any point on a string can be expressed as

$$\begin{cases} V_1(x,\omega) = -\frac{i f_1 \mathrm{e}^{ikx} \left(G^{-\frac{3}{2}} - 2G^{-\frac{1}{2}} \right)}{4kT}, \\ V_2(x,\omega) = V_3(x,\omega) = V_4(x,\omega) = \frac{i f_1 \mathrm{e}^{ikx} G^{-\frac{3}{2}}}{4kT}. \end{cases} \tag{24}$$

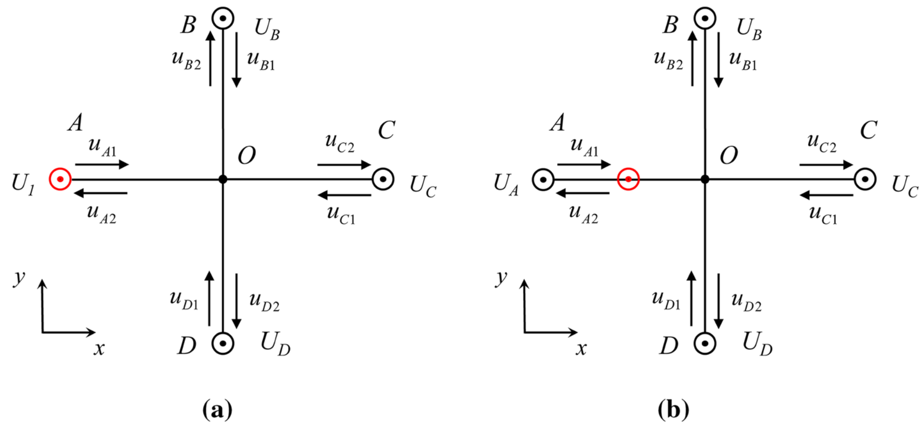

Fig. 4 Orthogonal cross-string structures with a different number of controllers. **a** The displacement excitation U_1 is at the boundary point A, and the controllers are set at the other three boundary points. **b** The excitation force f_1 is at the middle of string AO, and the controllers are set at all the boundary points

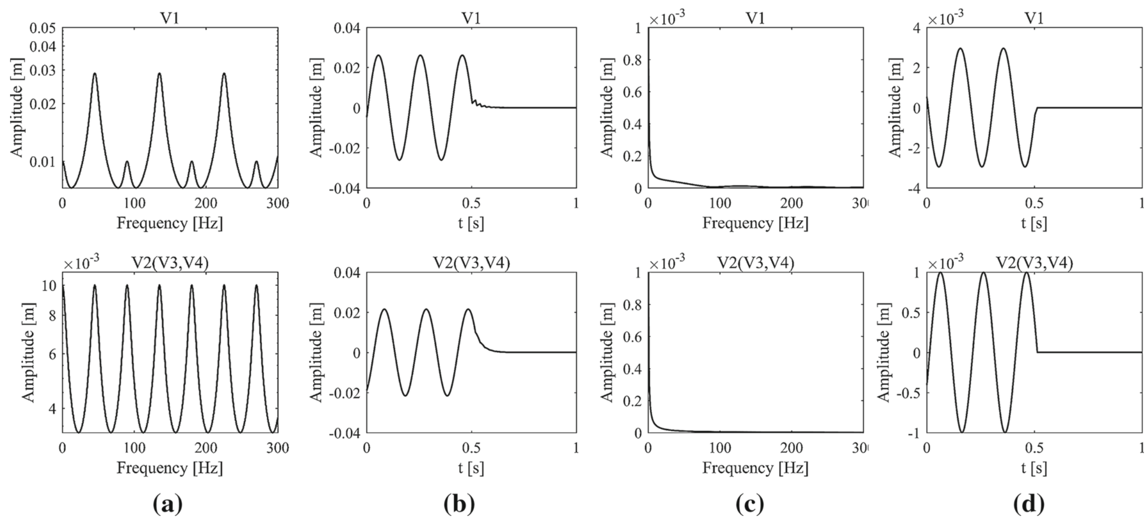

Fig. 5 Responses of the orthogonal cross-string structures. **a**, **b** The frequency-domain and time-domain responses of the structure with three controllers. **c**, **d** Frequency-domain and time-domain responses of the structure with four controllers at boundary points

According to the previous analysis, the term $1/(1-2G^2)$ in Eq. (21) can be expressed as Taylor series expansion and the $G^{-\frac{3}{2}}$ and $G^{-\frac{1}{2}}$ in Eq. (24) represent time delay. Therefore, there will be no residual vibration in the structures in Figs. 4a, b. However, in Fig. 5a, we can see that the time-domain frequency response of V_1 is larger than that of V_2, V_3, and V_4 because of the excitation boundary point A. Compared to this, when WBC controllers are set at all boundaries, the dynamic responses for all the strings can quickly reduce to zero without any residual vibration. In addition, by using the inverse Fourier transform, when its frequency response can be expressed in the form of $1/(1 \pm \delta G^n)$, $(\delta \neq 1)$, the structural vibrations will be gradually suppressed and reach stability eventually due to the convergent series. On the contrary, there will exist residual vibration in a string when the term $1/(1 \pm G^n)$ exists in its frequency response expression. The inverse Fourier transform method can be used not only to confirm the stability of the controlled structure but also to clearly demonstrate the physical mechanism of WBC method. By using our proposed WBC method, the poles of the net structure in the frequency domain are eliminated. Structural vibration (standing wave) is tailored into traveling waves with attenuated amplitude $(1/\delta)^n$.

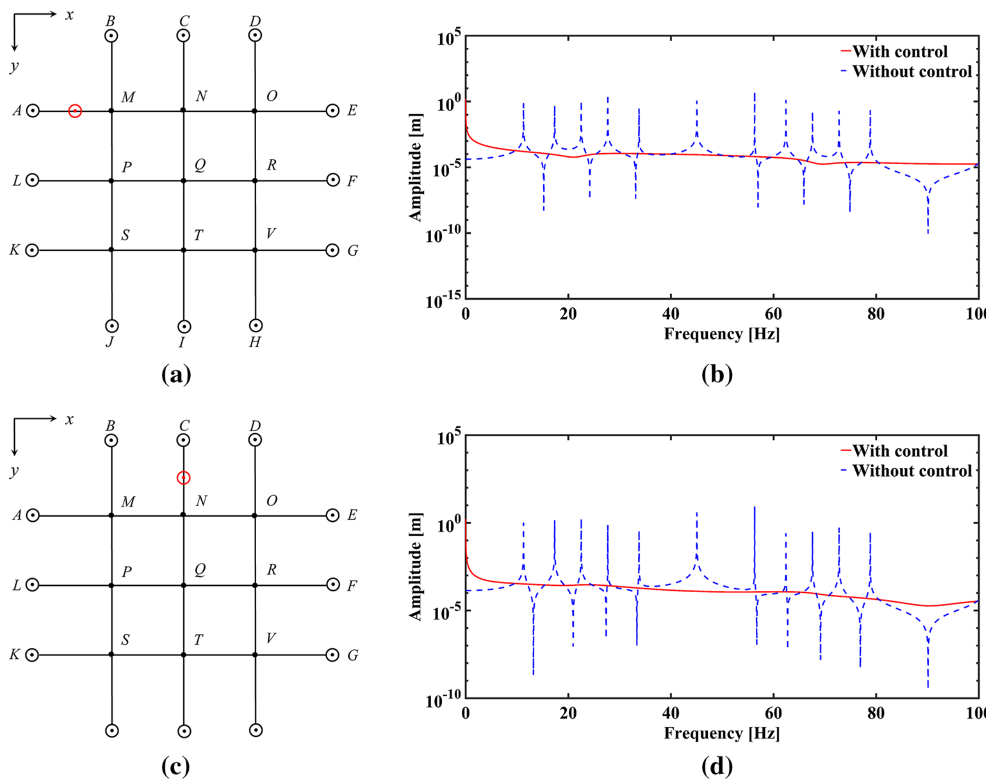

Fig. 6 Excitation acted at different locations. **a** The frequency response of the 3×3 net structure when an out-of-plane excitation is applied at the middle of the string AM. **b** The frequency response of the 3×3 net structure when an out-of-plane plane excitation is applied at the middle of the string CN

2.3 Orthogonal net structures with an excitation in boundary strings

The following investigation focuses on the stability of the net structures with controllers set at all the boundary points. For undamped net structures, the stability of the system means that the vibration of the structure can be controlled, that is, the structure can recover the stable state after a disturbance is removed. If the system is unstable, there will be residual vibration in the structure. For complex net structures, the response in the time domain cannot be obtained directly by inverse Fourier transform. Here, we can analyze the stability of the transfer functions under boundary excitations. The transfer functions of the system are the relation functions between the response and excitation of the system in the s domain. In classical control theory, the stability of the system can be judged by calculating the poles of the transfer functions. If the poles of the system transfer function have negative real parts, it can be determined that the system is stable.

The process of dynamic analysis for the net structure is the same as the orthogonal cross-string structure above. In this part, 3×3 net structure as shown in Fig. 6a is taken as an example to illustrate the stability analysis of complex net structures. For the structure mentioned in Fig. 2a, stability can also be studied through pole analysis.

We choose the string PQ in the 3×3 net structure to show its transfer function explicitly, while the others are in similar forms. The response of string PQ in the frequency domain can be obtained:

$$U_{PQx}(x,\omega) = -\frac{if_1\left(4\mathrm{e}^{-ikx}G^{\frac{1}{2}} + \mathrm{e}^{-ikx}G^{-\frac{3}{2}} - \mathrm{e}^{-ikx}G^{-\frac{7}{2}}\right)}{16(2G^2+1)Tk}, \tag{25}$$

where f_1 means a small external excitation at the middle of string AM and T is the initial tension. x is the distance to the point P along the string.

The pole of the transfer function is only related to denominator of the transfer function, and the denominator of the transfer function in the s domain can be expressed as

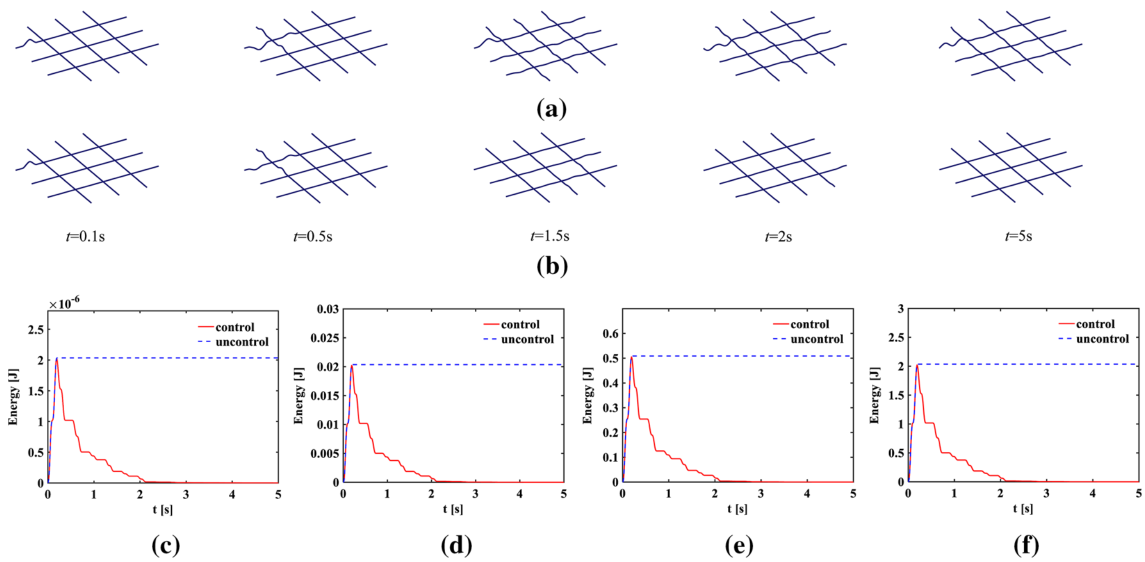

Fig. 7 Out-of-plane displacement responses simulated by the Lax–Friedrichs scheme of the whole structure at different time. **a** No control. **b** Boundary control. **c** Comparison of the total energy of the net structure. The parameters in each string are the same. The amplitude of the excitation in (**d**)–(**f**) is 1, 5, and 10, respectively

$$P(s) = 16\left(2e^{2s\frac{L}{c}} + 1\right)Ts, \tag{26}$$

where c and L are wave velocity and the length of per string, respectively.

All poles of the system can be obtained by solving $P(s) = 0$:

$$0,\ \frac{c}{2L}[(-0.693 + \pi \cdot i) + K \cdot 2\pi \cdot i], \quad (K = 0, 1, 2, 3, \ldots). \tag{27}$$

From the above solutions, we can see that transfer functions have only a zero-pole and infinitely complex poles with a negative real part, which represents the rigid mode and the flexible modes with damping, respectively. The poles analysis indicates that the system will be finally stable when no rigid mode is excited. Thus, the wave boundary control has a good effect on the vibration control of the net structure when the disturbance comes from the boundary strings.

For example, the net structure is assumed to be made of nylon strings whose material properties are as follows: The Young's modulus $E = 2.83$ GPa and the length density $\rho = 3.61\text{kg/m}^3$. In Fig. 6, $L = 0.245$ m and the initial tension T of the string is set to $1.75N$. A small external excitation $f_1 = 0.01$N is located at the midpoint of the string AM and the string CN as shown in Fig. 6, respectively. The responses of this net structure with control and without control are compared in Fig. 6. The frequency range varies from 0 to 100Hz. A conclusion can be drawn that the net structure can resist the formation of vibration induced by the excitation from the external boundary when the wave boundary control strategy is adopted.

A numerical analysis of the net structures is also investigated by the Lax–Friedrichs scheme (LFS) [20,42] in MATLAB. The LFS was first proposed [42] to investigate the numerical solution of hyperbolic partial differential equations, which is an FTCS (forward in time, centered in space) method. It is explicit and first-order accurate in time and first-order accurate in space, provided that the initial values and boundary values are sufficiently smooth functions. A small external force excitation is located at the midpoint in string AM whose values are $f_1(t) = 0.01\sin(10\pi t)(0 < t \leq 0.2\,\text{s})$ and $f_1(t) = 0(t > 0.2\,\text{s})$. The amplitude of force is 0.01 N. All the strings have no initial displacement and velocity. The black and red circles represent the controllers and the force excitation, respectively.

Figures 7a, b show the dynamic responses of the whole net structure without and with control at time $t = 0.1$ s, 0.5 s, 1.5 s, 2 s, and 5 s. Figures 7c–f present the total energy of the net structure for different amplitudes of excitation, name 0.01, 1, 5, and 10, respectively. The excitation acted at string AM produces traveling waves in two directions. One direction of the wave travels to the boundary point A, and the other direction of the wave propagates into the structure. Because of the boundary controllers, the traveling wave reaching the boundary will be eliminated without reflecting. As transmission and reflection through the interior of the structure, all traveling waves will be eliminated ultimately. The total energy of the 3×3 net structure under no control and wave boundary control is calculated by the trapezoidal rule [34] (see Appendix B). As Fig. 7c depicts, in the beginning, the total energy increases due to the work done by the force excitation. When the boundary controllers work, the total energy of the whole structure decreases to zero. The boundary controllers resist the formation of vibration induced by excitation from the external boundary. Compared to this, in the uncontrolled case, the total energy will maintain a stable value, where standing waves are formed in the net structure. Figures 7d–f indicate that the effectiveness of the controller was demonstrated for an arbitrary initial excitation of the net structure. The time to achieve the stability of the structure changes little with increasing amplitude of excitation. The results show that the vibration suppression is more effective for large initial energies.

3 Different control laws for net structures

3.1 Control laws corresponding to different observations

In this subsection, the control laws corresponding to different observations are derived and the relationship between common observations and control quantities is summarized. A 5×5 net structure is shown in Fig. 8a, where a controller and a sensor are set on the two ends of every boundary string. As Fig. 8 shows, the cylinders represent the controllers and the rhombuses express the observations. The observations can be measured by non-contact laser sensors. The selection of the sensor is related to the measured position and vibration frequency. It is generally believed that in low-frequency range, the vibration intensity is proportional to the displacement. In intermediate-frequency range, the vibration intensity is proportional to the velocity, while it is proportional to the acceleration in high-frequency range. Thus, in this paper, the displacement observation is mainly adopted because the displacement response of the net structure is quite small. Due to the boundary control, the waves propagate to the structural boundary and will eventually be eliminated by the controller. For the controlled case, the derivation of the control law is similar to a single string as shown in Fig. 8b.

In Fig. 8b, we select the force as the control quantity and the observation is displacement, force, velocity, and acceleration, respectively. As we know, the force control F_c at the left point a needs to satisfy the force balance condition:

$$-i \cdot k \cdot T \cdot u_l^1 + i \cdot k \cdot T \cdot u_r^1 + F_c = 0. \tag{28}$$

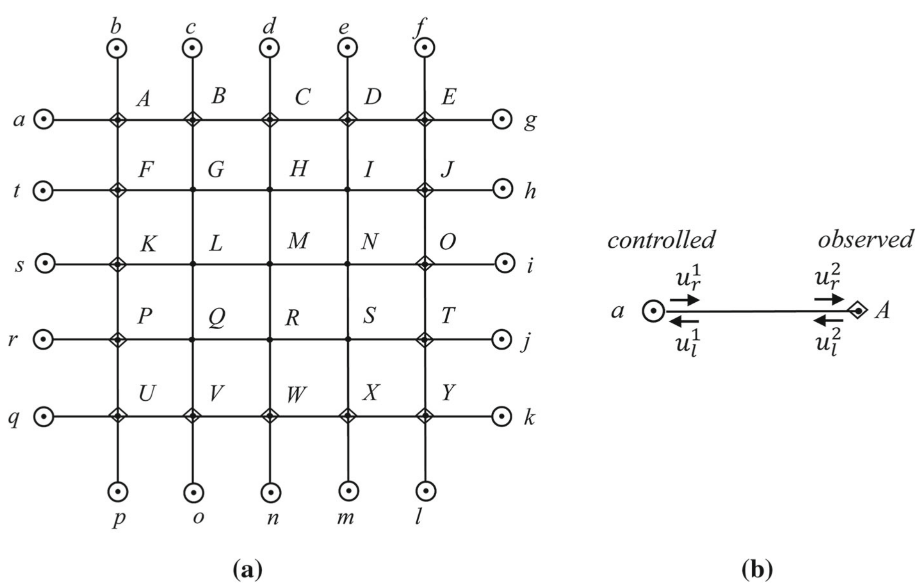

Fig. 8 The 5×5 net structure. **a** The model with controllers and sensors on its boundary strings. **b** The substructure with a controller and a sensor

On the right point A, the sensor measures the superposition of two directional traveling waves, which can be expressed as

$$U_{\mathrm{s}} = u_{\mathrm{l}}^{2} + u_{\mathrm{r}}^{2}. \tag{29}$$

According to the traveling wave continuous condition and the reflected wave $u_{\mathrm{r}}^{1} = 0$,

$$\begin{cases} u_{\mathrm{l}}^{1} = u_{\mathrm{l}}^{2} \cdot \mathrm{e}^{-ikL}, \\ u_{\mathrm{r}}^{1} = u_{\mathrm{r}}^{2} \cdot \mathrm{e}^{ikL}, \\ u_{\mathrm{r}}^{1} = 0. \end{cases} \tag{30}$$

Substituting Eq. (30) into Eqs. (28) and (29), we can obtain the expression of the control law:

$$F_{\mathrm{c}} = -i \cdot k \cdot T \cdot U_{\mathrm{s}} \cdot \mathrm{e}^{-ikL}, \tag{31}$$

which is the same as Eq. (7). Thus, control laws corresponding to different observations can be obtained by the same derivation process. Substituting Eq. (31) into Eq. (28) and resolving Eqs. (28)–(30), one can obtain the traveling waves in the structure. The displacement of an arbitrary point $V(x)$ on the string in its local coordinate system can be expressed as

$$V(x, \omega) = u_{\mathrm{l}}^{2} \cdot \mathrm{e}^{-ikx} + u_{\mathrm{r}}^{2} \cdot \mathrm{e}^{ikx} = \mathrm{e}^{-ikx} U_{\mathrm{s}}, \tag{32}$$

where x means distance to the sensor. When $x = L$, namely at the position of the controller, $V(L, \omega) = \mathrm{e}^{-ikL} U_{\mathrm{s}}$. The waves propagate to the controller stably without reflecting waves. Similarly, we adopt the control law $U_c = \mathrm{e}^{-ikL} U_{\mathrm{s}}$ derived in Eq. (6), and the displacement of an arbitrary point $V(x)$ on the string can be also expressed as $V(x, \omega) = \mathrm{e}^{-ikx} U_{\mathrm{s}}$ which is the same as Eq. (32). The results indicate that the expressions of the displacement are the same though the observations are different.

When the controls and the observations are force F_{c} and F_S, respectively, we can get the equations about the traveling wave component, control, and the observation as follows:

$$\begin{cases} -i \cdot k \cdot T \cdot u_{\mathrm{r}}^{1} + i \cdot k \cdot T \cdot u_{\mathrm{l}}^{1} + F_{\mathrm{c}} = 0, \\ i \cdot k \cdot T \cdot u_{\mathrm{r}}^{1} \cdot \mathrm{e}^{-ikL} - i \cdot k \cdot T \cdot u_{\mathrm{l}}^{1} \cdot \mathrm{e}^{ikL} = F_{\mathrm{s}}. \end{cases} \tag{33}$$

Then, the control law is obtained:

$$F_{\mathrm{c}} = F_{\mathrm{s}} \cdot \mathrm{e}^{-ikL}. \tag{34}$$

If the observation is the velocity V_{s}, the equations become the following formula:

$$\begin{cases} -i \cdot k \cdot T \cdot u_{\mathrm{r}}^{1} + i \cdot k \cdot T \cdot u_{\mathrm{l}}^{1} + F_{\mathrm{c}} = 0, \\ u_{\mathrm{r}}^{1} \cdot \mathrm{e}^{-ikL} + u_{\mathrm{l}}^{1} \cdot \mathrm{e}^{ikL} = U_{\mathrm{s}}. \end{cases} \tag{35}$$

Then, the control law becomes as follows:

$$F_{\mathrm{c}} = -\frac{k \cdot T}{\omega} \cdot V_{\mathrm{s}} \cdot \mathrm{e}^{-ikL}. \tag{36}$$

In the same way, the acceleration can also be chosen as the observation, and the equations become as follows:

$$\begin{cases} -i \cdot k \cdot T \cdot u_{\mathrm{r}}^{1} + i \cdot k \cdot T \cdot u_{\mathrm{l}}^{1} + F_{\mathrm{c}} = 0, \\ -\omega^{2} \cdot u_{\mathrm{r}}^{1} \cdot \mathrm{e}^{-ikL} - \omega^{2} \cdot u_{\mathrm{l}}^{1} \cdot \mathrm{e}^{ikL} = a_{\mathrm{s}}. \end{cases} \tag{37}$$

So the control law can be expressed as

$$F_{\mathrm{c}} = -\frac{i \cdot k \cdot T}{\omega^{2}} \cdot a_{\mathrm{s}}. \cdot \mathrm{e}^{-ikL}. \tag{38}$$

The control laws corresponding to different observations are summarized in Table 1. The derivation process is exactly the same as Sect. 3.1. Through the calculation results in this section, we can know that no matter what control law is adopted, the expression of displacement of an arbitrary point on the string is same when the observations are the same (see Table 2 in Appendix C).

Table 1 Control laws of different observations and controls

Observations/controls	Displacement	Force	Velocity	Acceleration
Displacement	$U_C = \mathrm{e}^{-ikl} U_S$	$F_C = -ikT\mathrm{e}^{-ikl} U_S$	$V_C = -i\omega\mathrm{e}^{-ikl} U_S$	$A_C = \omega^2\mathrm{e}^{-ikl} U_S$
Force	$U_C = \frac{i}{kT}\mathrm{e}^{-ikl} F_S$	$F_C = \mathrm{e}^{-ikl} F_S$	$V_C = -\frac{\omega}{kT}\mathrm{e}^{-ikl} F_S$	$A_C = -\frac{i\omega^2}{kT}\mathrm{e}^{-ikl} F_S$
Velocity	$U_C = -\frac{i}{\omega}\mathrm{e}^{-ikl} V_S$	$F_C = -\frac{kT}{\omega}\mathrm{e}^{-ikl} V_S$	$V_C = -\mathrm{e}^{-ikl} V_S$	$A_C = -i\omega\mathrm{e}^{-ikl} V_S$
Acceleration	$U_C = -\frac{1}{\omega^2}\mathrm{e}^{-ikl} A_S$	$F_C = -\frac{ikT}{\omega^2}\mathrm{e}^{-ikl} A_S$	$V_C = -\frac{i}{\omega}\mathrm{e}^{-ikl} A_S$	$A_C = -\mathrm{e}^{-ikl} A_S$

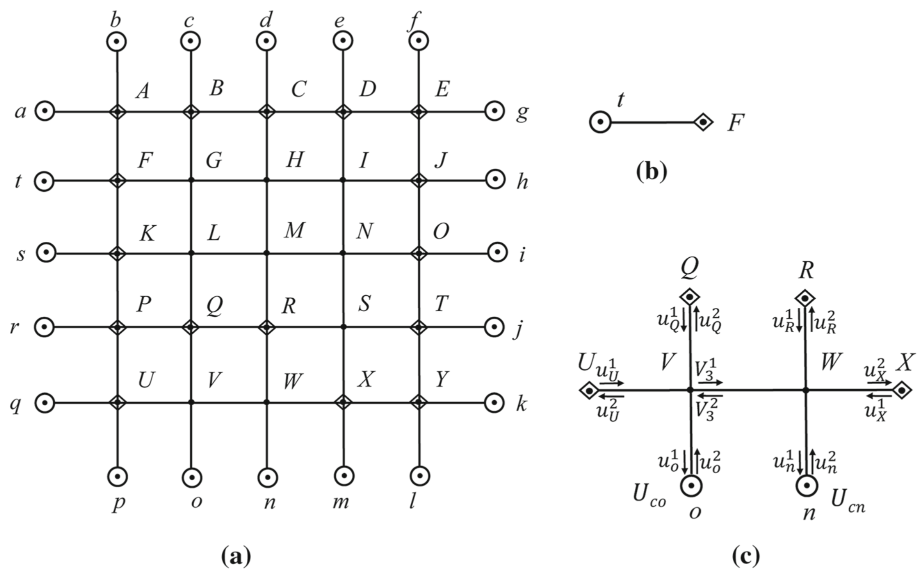

Fig. 9 A 5 × 5 net structure. **a** The distribution of sensors; **b**, **c** two types of substructures

3.2 Control laws corresponding to the distribution of sensors

For wave boundary control, as long as controllers are applied on every boundary string, the control law can be obtained even if the structure is very complex. According to the different positions of sensors, different boundary control laws can be obtained. For example, for the 5×5 net structure, different distributions of sensors model can be designed where the total number of sensors remains equal to the quantity of the boundaries. When force or acceleration sensors are adapted, the control laws can be obtained easily by the similar derivation process as Sect. 2. It is noted that, as long as displacement sensors are adapted, the whole net structure can be considered as several substructures according to the displacement continuity conditions at junctions. The control laws need to be derived on the substructures. For example, in Fig. 9a, when we adopt the displacement observation, the structure can be divided into two types of substructures as shown in Figs. 9b, c. Figure 9b is the model of a single string as the same as Fig. 8b. Thus, its control law is the same as Eq. (6) (or check in Table 1).The control law for the configuration in Fig. 9c can also be derived as follows (the displacement at the joint point U, Q, R, X in Fig. 9c can be measured by the sensors):

$$\begin{cases} u_U^1 + u_U^2 = U_\mathrm{s}, \\ u_Q^1 + u_Q^2 = Q_\mathrm{s}, \\ u_R^1 + u_R^2 = R_\mathrm{s}, \\ u_X^1 + u_X^2 = X_\mathrm{s}, \\ u_o^1 + u_o^2 = U_\mathrm{co}, \\ u_n^1 + u_n^2 = U_\mathrm{cn}, \end{cases} \tag{39}$$

where U_s, Q_s, R_s, and X_s represent the displacement values measured by sensors. U_co and U_cn represent the boundary control laws for the substructure in Fig. 9c.

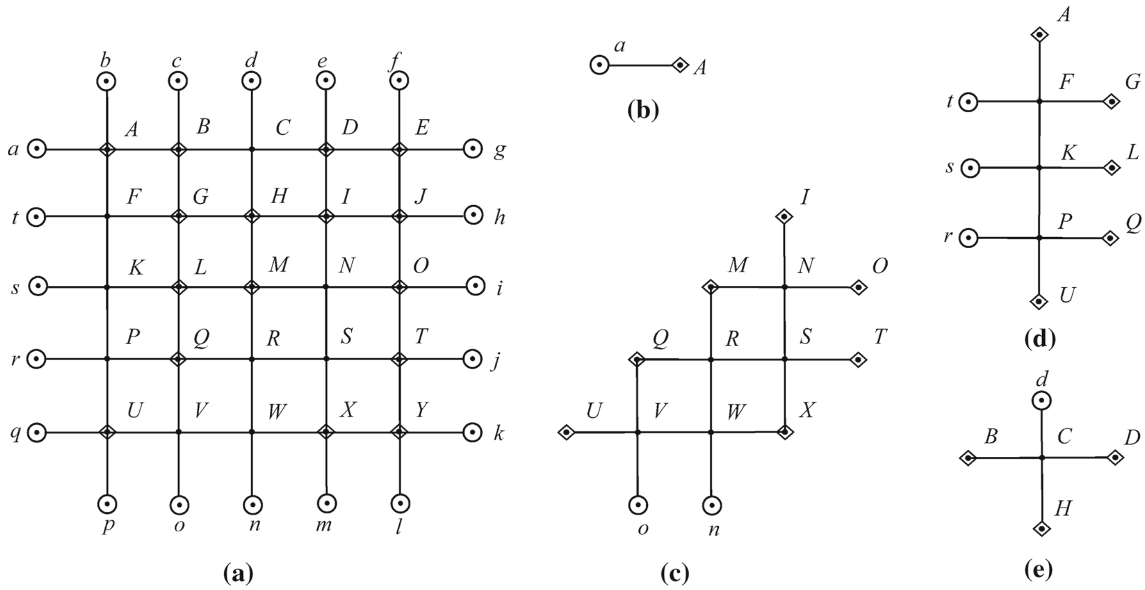

Fig. 10 A 5 × 5 net structure: **a** the distribution of sensors; **b**–**e** the four types of substructures

According to displacement continuity conditions and force equilibrium equations at junction V and W, traveling wave components can be obtained. Besides, the wave boundary control theory requires the boundary reflected waves $u_o^2 = 0$ and $u_n^2 = 0$. Then, the control laws can be obtained as follows:

$$\begin{cases} U_{\mathrm{co}} = \frac{U_{\mathrm{s}}(1+2G^2)+Q_{\mathrm{s}}(1+2G^2)+(R_{\mathrm{s}}+X_{\mathrm{s}})G}{1+3G^2+4G^4}, \\ U_{\mathrm{cn}} = \frac{(U_{\mathrm{s}}+Q_{\mathrm{s}})G+(R_{\mathrm{s}}+X_{\mathrm{s}})(1+2G^2)}{1+3G^2+4G^4}. \end{cases} \tag{40}$$

By distributing sensors in this case, the net structure in Fig. 9a will be stable when the boundary control laws Eqs. (6) and (40) are adopted.

The sensor position can also be designed as shown in Fig. 10a. When we adopt the displacement observation, the net structures can be divided into four types of substructures as shown in Figs. 10b–e. The controllers are set at the boundary points, and the derivation process of control laws is the same as Eqs. (39) to (40).

The boundary control laws for the net structures in Fig. 10a are

$$\begin{cases} U_{ca} = A_{\mathrm{s}} G^{-1}, \\ U_{cd} = \frac{B_{\mathrm{s}}+D_{\mathrm{s}}+H_{\mathrm{s}}}{1+2G^2}, \\ U_{ct} = \frac{(1+3G^2+4G^4)(A_{\mathrm{s}}+G_{\mathrm{s}})+G(1+2G^2)L_{\mathrm{s}}+G^2(Q_{\mathrm{s}}+U_{\mathrm{s}})}{1+4G^2+8G^4+8G^6}, \\ U_{cs} = \frac{(1+2G^2)L_{\mathrm{s}}+G(A_{\mathrm{s}}+G_{\mathrm{s}}+Q_{\mathrm{s}}+U_{\mathrm{s}})}{1+4G^2+8G^4+8G^6}, \\ U_{cr} = \frac{(1+3G^2+4G^4)(Q_{\mathrm{s}}+U_{\mathrm{s}})+G(1+2G^2)L_{\mathrm{s}}+G^2(A_{\mathrm{s}}+G_{\mathrm{s}})}{1+4G^2+8G^4+8G^6}, \\ U_{\mathrm{co}} = \frac{1}{\alpha}\left[\beta U_{\mathrm{s}} + \gamma Q_{\mathrm{s}} + (4G^2+8G^4+4G^6)M_{\mathrm{s}} + G^4(I_{\mathrm{s}}+O_{\mathrm{s}}) + (4G^3+4G^5)T_{\mathrm{s}} + \eta X_{\mathrm{s}}\right], \\ U_{\mathrm{cn}} = \frac{1}{\alpha}[\eta U_{\mathrm{s}} + \lambda Q_{\mathrm{s}} + \psi M_{\mathrm{s}} + (G^3+2G^5)(I_{\mathrm{s}}+O_{\mathrm{s}}) + (4G^2+12G^4+8G^6)T_{\mathrm{s}} + \gamma X_{\mathrm{s}}], \end{cases} \tag{41}$$

where the U_{s}, Q_{s}, M_{s}, I_{s}, O_{s}, T_{s}, and X_{s} represent the displacement values measured by sensors and the expressions α, β, γ, η, λ, ψ are in Appendix A.9.

By comparing the two examples, we can see that the sensors' position has an important influence on the control laws for the net structure. The sensors can be arranged in reasonable positions depending on the usage demand, and the control laws are also required to be amended according to our method.

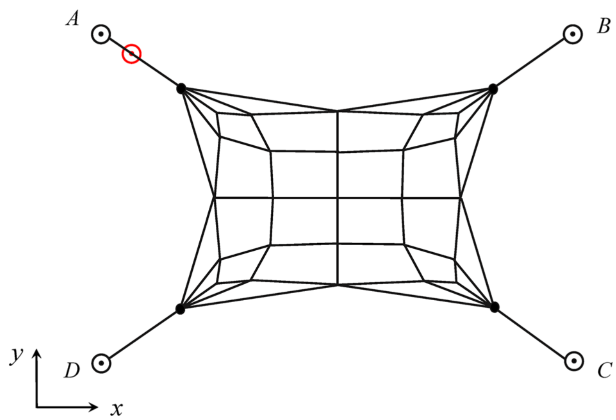

Fig. 11 A net structure reducing the boundaries. The locations of the wave-based boundary controllers and a small force excitation: the black circles, red circles, and black points represent the controllers, the force excitation, and sensors, respectively (colour figure online)

4 Application for reducing the number of boundaries and controllers

In the previous sections, the effectiveness of wave boundary control for external excitation on the boundary is verified theoretically and numerically. As we know, in traditional modal control, the number of needed controllers is related to the considered modes. The larger the structure is, the more the controllers are needed. Especially for large flexible net structures, the models are such dense and numerous that the required number of controllers is huge. The wave boundary control method we proposed requires the number of controllers only equal to the number of boundaries. Here, we put forward an innovative way to reduce the number of controllers by weaving design boundaries. In this subsection, the shape finding algorithm method based on force density method (FDM) [43] is applied to design a new configuration of the net structure depicted in Fig. 11. In the shape finding analysis by the FDM, the boundary points A, B, C, D are the fixed nodes that the position coordinates are (0,2), (2,2), (2,0), (0,0). The other nodes are the free nodes, represented by (x_f, y_f) and (x, y), respectively. The force density vector $\boldsymbol{q} = [q_1\ q_2\ q_3\ q_4\ q_5 \ldots q_m]^{\mathrm{T}}$ among m means the total number of the strings in the whole structure. Here, the force density of the four boundary strings is equal to 5, and that of the other strings in the structure is equal to 1. Next, the topological matrix $\boldsymbol{C}_{\mathrm{s}}$ is defined by

$$C_{\mathrm{s}} = \begin{cases} +1 & \text{if } q = \min(i, j), \\ -1 & \text{if } q = \max(i, j), \\ 0 & \text{for other cases,} \end{cases} \tag{42}$$

where all of the strings and nodes in the net are in an arbitrary order, supposing the string matches node i and node j. Then, the position coordinates x, y of free nodes in the net structure can be solved by applying the FDM [44,45]. The material properties of the net structure are listed in Sect. 2.3. A small external force excitation is located at the red circle which is the 1/5 length of the string aA whose value is $f_1(t) = 0.01 \sin(10\pi t)(0 < t \leq 0.2\,\mathrm{s})$ and $f_1(t) = 0(t > 0.2\,\mathrm{s})$. All the strings have no initial displacement and velocity. Numerical analysis of the net structure with reduced boundary is investigated by the Lax–Friedrichs scheme (LFS) [20,42] in MATLAB.

Only four boundary controllers are used for the net structure in the full frequency range, and the boundary control law is still $U_C = \mathrm{e}^{-ikl} U_S$. In Fig. 12, dynamic responses represent the out-of-plane displacement at time $t = 0.1$ s, 1.5 s, 15 s, and 180 s. When $t = 0.1$ s, the external excitation (red circle) produces traveling waves that travel in two directions. At $t = 1.5$ s, the wave propagates into the structure (Fig. 12). As the time increases to 15 s, for the uncontrolled case (Fig. 12a), the waves almost spread all over the structure and reflected waves are formed on the boundary. At $t = 180$ s, the vibration on the structure has been generated. By contrast, we can see that the waves propagate to boundaries and are finally eliminated by the boundary controllers. Therefore, there are no reflected waves when the controllers are applied at the boundary strings (Fig. 12b). Namely, the boundary controllers resist the formation of vibration induced by excitation from the external boundary. Figure 13a shows the control inputs with increasing time t. Figure 13b shows the total energy of the net structure for the two cases. In the uncontrolled case, the total energy finally maintains a

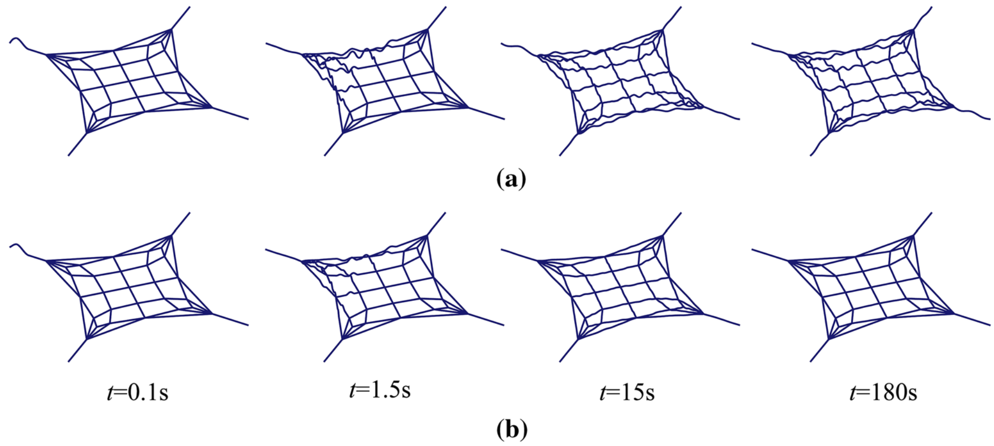

Fig. 12 A comparison of the out-of-plane displacement simulated by the LFS of the whole structure at the different time that the parameters in each string are different. **a** No control; **b** wave boundary control strategy

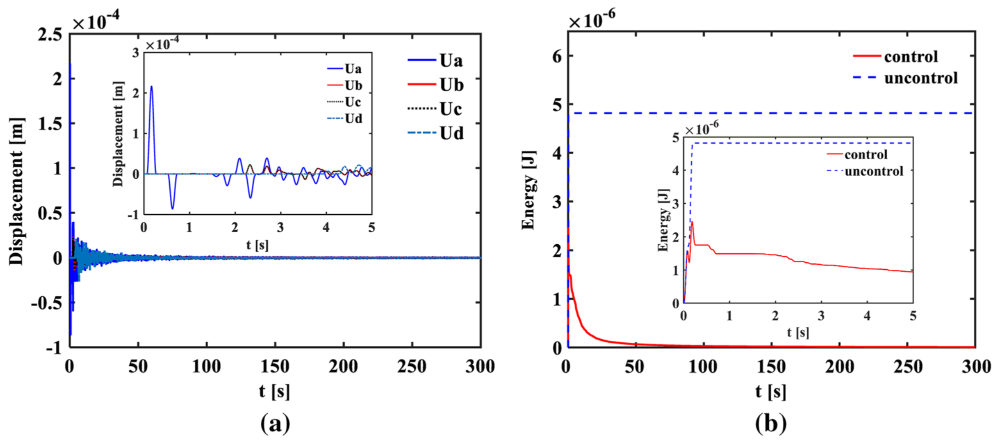

Fig. 13 **a** Control inputs of the U_a, U_b, U_c, and U_d. **b** Comparison of the total energy of the net structure

stable value. In contrast to the uncontrolled case, the total energy of the whole structure decreases to zero because the controllers eliminate the waves propagating to the boundaries, indicating that there is no residual item. Compared with the modal control method, the wave boundary control is available in the full frequency domain. Modal truncation is not required, and modal spillover can also be avoided. Therefore, our proposed method can greatly reduce the number of controllers and it is an effective way to achieve structural stability in engineering.

5 Conclusions

In this paper, a wave boundary control (WBC) strategy is proposed for vibration control on large net structures. The stability of the controlled structure is confirmed by using inverse Fourier transform, transfer function analysis, and numerical simulation. When WBC controllers are set at all boundaries and excitation comes from the boundary, dynamic responses for all the strings can reduce to zero without any residual vibration. The physical mechanism is that the poles of the net structure in the frequency domain are eliminated by using our proposed WBC method, and further structural vibration (standing wave) is tailored into traveling waves. In addition, the different sensors can be arranged in reasonable positions depending on the usage demand, and the corresponding control laws can also be derived based on our method. As an application on large net structures, we propose to reduce the number of controllers by weaving design boundaries which can provide a new avenue for vibration control on large net structures. In the future, the nonlinear vibration control strategy for large net structures based on wave theory will be considered. Meanwhile, the control strategy based on wave theory and the efficiency comparison with other vibration control strategies are also worth studying.

Acknowledgements The authors thank Xinwei Xu for the help in the theoretical work. This work was supported by the National Natural Science Foundation of China [Grant Nos. 11290153 and 11672037].
Author contributions KZ proposed the key idea of this paper. SLZ and KZ developed the analytical method and carried out the numerical computation. YL assisted with the building of the numerical program. GKH assisted with discussing the results. SLZ, KZ, and GKH contributed to the writing of the paper.

Appendix A

Wave boundary control laws for the model in Fig. 3a:

$$U_C = \frac{U_1}{2G^2}, \quad U_D = \frac{U_1}{2G^2}. \tag{A.1}$$

The traveling waves at the boundary points can be expressed as

$$\begin{cases} u_{A1} = \frac{U_1(1-2G^2)}{2-2G^2}, \quad u_{A2} = \frac{U_1}{2-2G^2}, \\ u_{B1} = \frac{U_1}{2-2G^2}, \quad u_{B1} = -\frac{U_1}{2-2G^2}, \\ u_{c1} = 0, \quad u_{C2} = \frac{U_1}{2G^2}, \\ u_{D1} = 0, \quad u_{D2} = \frac{U_1}{2G^2}. \end{cases} \tag{A.2}$$

Thus, the frequency responses for Fig. 3a can be obtained as

$$\begin{cases} V_1(x,\omega) = \frac{\mathrm{e}^{-ikx}(1-2G^2+\mathrm{e}^{2ikx})U_1}{2(1-G^2)}, \\ V_2(x,\omega) = \frac{\mathrm{e}^{-ikx}(1-\mathrm{e}^{2ikx})U_1}{2(1-G^2)}, \\ V_3(x,\omega) = \frac{\mathrm{e}^{ikx}U_1}{2G^2}, \quad V_4(x,\omega) = \frac{\mathrm{e}^{ikx}U_1}{2G^2}, \end{cases} \tag{A.3}$$

$$V_3(x,t) = V_4(x,t) = \frac{1}{2}U_1\left(t - 2\frac{l}{c} + \frac{x}{c}\right). \tag{A.4}$$

Similarly, for the three controllers model in Fig. 4a, the control laws are

$$U_B = \frac{U_1}{2G^2-1}, \quad U_C = \frac{U_1}{2G^2-1}, \quad U_D = \frac{U_1}{2G^2-1}. \tag{A.5}$$

The traveling waves at boundary points for Fig. 4a can be expressed as

$$\begin{cases} u_{A1} = -\frac{2G^2U_1}{1-2G^2}, \quad u_{A2} = \frac{U_1}{1-2G^2}, \\ u_{B1} = 0, \quad u_{B1} = -\frac{U_1}{1-2G^2}, \\ u_{c1} = 0, \quad u_{C2} = -\frac{U_1}{1-2G^2}, \\ u_{D1} = 0, \quad u_{D2} = -\frac{U_1}{1-2G^2}, \end{cases} \tag{A.6}$$

The time responses for the three controllers model in Fig. 4a are as follows:

$$\begin{cases} V_1(x,t) = -\sum\limits_{n=0}^{\infty} \frac{1}{2^{n+1}}U_1\left(t - \frac{2(n+1)l}{c} + \frac{x}{c}\right) + \sum\limits_{n=0}^{\infty} \frac{1}{2^n}U_1\left(t - \frac{2nl}{c} - \frac{x}{c}\right), \\ V_2(x,t) = V_3(x,t) = V_4(x,t) = \sum\limits_{n=0}^{\infty} \frac{1}{2^{n+1}}U_1\left(t - \frac{2(n+1)l}{c} + \frac{x}{c}\right). \end{cases} \tag{A.7}$$

The time responses for the four controllers model in Fig. 4b are as follows:

$$\begin{cases} V_1(x,t) = -\frac{i}{4kT}\left[f_1\left(t-\frac{3l}{2c}+\frac{x}{c}\right)-2f_1\left(t-\frac{l}{2c}+\frac{x}{c}\right)\right], \\ V_2(x,t) = V_3(x,t) = V_4(x,t) = \frac{i}{4kT}f_1\left(t-\frac{3l}{2c}+\frac{x}{c}\right), \end{cases} \tag{A.8}$$

$$\begin{cases} \alpha = (8+40G^2+97G^4+130G^6+96G^8+32G^{10}), \\ \beta = 8+32G^2+53G^4+44G^6+16G^8, \\ \gamma = 8+36G^2+60G^4+48G^6+16G^8, \\ \eta = 8G+20G^3+20G^5+8G^7, \\ \lambda = 12G+35G^3+38G^5+16G^7, \\ \psi = 4G+16G^3+20G^5+8G^7. \end{cases} \tag{A.9}$$

Appendix B

The total energy of the net structure is the sum of the kinetic and the energy of each string. The energy of the string is as follows:

$$E(t) = \frac{1}{2}\int_0^L (\rho\,|V_t(x,t)|^2 + T\,|V_x(x,t)|^2)\mathrm{d}x. \tag{B.1}$$

The space interval [0, L] is the length of the string and discretized into m equally spaced panels. By applying the trapezoidal rule to each panel, the approximation to the energy of this string (Eq. (B.1)) at time t_q becomes

$$E(t_q) = \frac{1}{2}\sum_{p=0}^{(m-1)L}\int_{p\Delta x}^{(p+1)\Delta x} (\rho\,\left|V_t(x,t_q)\right|^2 + T\,\left|V_x(x,t_q)\right|^2)\mathrm{d}x. \tag{B.2}$$

After a summation of $E(t_q)$ for all strings, we can obtain the total energy of the net structure at time t_q.

Appendix C

The expression of the displacement of an arbitrary point on the string (see Fig. 1 or Fig. 8b) corresponding to different observations is shown in Table 2.

Table 2 Displacement of an arbitrary point on the string corresponding to different observations

Controls/observations	Displacement	Force	Velocity	Acceleration
Displacement/force/ velocity/acceleration	$V(x,\omega) = \mathrm{e}^{-ikx}U_\mathrm{s}$	$V(x,\omega) = \frac{i}{kT}\mathrm{e}^{-ikx}F_S$	$V(x,\omega) = -\frac{i}{\omega}\mathrm{e}^{-ikx}V_S$	$V(x,\omega) = -\frac{1}{\omega^2}\mathrm{e}^{-ikx}A_S$

References

1. Tibert, G.: Deployable Tensegrity Structures for Space Applications. Royal Institute of Technology, Stockholm (2002)
2. Zhang, Y., Li, N., Yang, G., Ru, W.: Dynamic analysis of the deployment for mesh reflector deployable antennas with the cable-net structure. Acta Astronaut. **131**, 182–189 (2017)
3. Zhang, W., Liu, T., Xi, A., Wang, Y.N.: Resonant responses and chaotic dynamics of composite laminated circular cylindrical shell with membranes. J. Sound Vib. **423**, 65–99 (2018)
4. Hu, H., Tian, Q., Zhang, W., Jin, D., Hu, G., Song, Y.: Nonlinear dynamics and control of large deployable space structures composed of trusses and meshes. Adv. Mech. **43**, 390–414 (2013)
5. Fuller, C.R., Elliott, S.J., Nelson, P.A.: Active Control of Vibration. Academic Press, London (1996)
6. Inman, D.J.: Control of Vibrations. Wiley, New York (2006)
7. Moshrefi-Torbati, M., Forrester, J.A., Forrester, A.I.J., Keane, A.J., Brennan, M.J., Elliott, S.J.: Novel active and passive anti-vibration mountings. J. Sound Vib. **331**, 1532–1541 (2012)
8. Gawronski, W.K.: Advanced Structural Dynamics and Active Control of Structures. Springer, New York (1998)
9. Wang, Z., Li, T.: Optimal Piezoelectric sensor/actuator placement of cable net structures using H2-norm measures. J. Vib. Control. **20**, 1257–1268 (2014)

10. Liu, F., Jin, D., Wen, H.: Optimal vibration control of curved beams using distributed parameter models. J. Sound Vib. **384**, 15–27 (2016)
11. Mace, B.R.: Wave reflection and transmission in beams. J. Sound Vib. **97**, 237–246 (1984)
12. Mace, B.R.: Active control of flexural vibrations. J. Sound Vib. **114**, 253–270 (1987)
13. Flotow, A.H.Von: Traveling wave control for large spacecraft structures. J. Guid. Control Dyn. **9**, 462–468 (1986)
14. Tanaka, N., Kikushima, Y.: Active wave control of a flexible beam (Proposition of the active sink method). JSME Int. J. **34**, 159–167 (1991)
15. Tanaka, N., Kikushima, Y.: Flexural wave control of flexible beam: fundamental characteristics of an active sink system and its verification. Trans. Jpn. Soc. Mech. Eng. Ser C **56**(530), 2575–2582 (1990)
16. Spadoni, A., Ruzzene, M., Cunefare, K.: Vibration and wave propagation control of plates with periodic arrays of shunted piezoelectric patches. J. Intell. Mater. Syst. Struct. **20**, 979–990 (2009)
17. Wu, Z.J., Li, F.M.: Spectral element method and its application in analysing the vibration band gap properties of two-dimensional square lattices. J. Vib. Control. **22**, 710–721 (2016)
18. Fujii, H.A., Watanabe, T., Taira, W., Trivailo, P.: An analysis of vibration and wave-absorbing control of tether systems. AIAA Guidance, Navigation, and Control Conference and Exhibit. AIAA2001-4033 (2001)
19. Wang, Z., Li, T.: Linear dynamic analysis and active control of space prestressed taut cable net structures using wave scattering method. Struct. Control Heal. Monit. **23**, 783–798 (2016)
20. Meirovitch, L., Baruh, H.: On the problem of observation spillover in self-adjoint distributed-parameter systems. J. Optim. Theory Appl. **39**, 269–291 (1983)
21. Logan, J.D.: Applied Mathematics. Wiley, New Jersey (2006)
22. O'Connor, W.J., Zhu, M.: Boundary-controlled travelling and standing waves in cascaded lumped systems. Mech. Syst. Signal Process. **39**, 119–128 (2013)
23. Habibi, H., O'Connor, W.J.: Wave-based control of planar motion of beam-like mass-spring arrays. Wave Motion. **72**, 317–330 (2017)
24. Kreuzer, E., Steidl, M.: Controlling torsional vibrations of drill strings via decomposition of traveling waves. Arch. Appl. Mech. **82**, 515–531 (2012)
25. Rad, H.K., Salarieh, H., Alasty, A., Vatankhah, R.: Boundary control of flexible satellite vibration in planar motion. J. Sound Vib. **432**, 549–568 (2018)
26. Krstic, M., Smyshlyaev, A.: Boundary Control of PDEs: A Course on Backstep. SIAM, Philadelphia (2008)
27. Wang, J., Tang, S., Pi, Y., Krstic, M.: Automatica Exponential regulation of the anti-collocatedly disturbed cage in a wave PDE-modeled ascending cable elevator. Automatica **95**, 122–136 (2018)
28. Wang, J., Pi, Y., Krstic, M.: Automatica Balancing and suppression of oscillations of tension and cage in dual-cable mining elevators. Automatica **98**, 223–238 (2018)
29. Zhao, Z., Wang, X., Zhang, C., Liu, Z., Yang, J.: Neural network based boundary control of a vibrating string system with input deadzone. Neurocomputing **275**, 1021–1027 (2018)
30. Zhao, Z., Shi, J., Lan, X., Wang, X., Yang, J.: Adaptive neural network control of a flexible string system with non-symmetric dead-zone and output constraint. Neurocomputing **283**, 1–8 (2018)
31. Zhao, Z., Liu, Z., Li, Z., Wang, N., Yang, J.: Control design for a vibrating flexible marine riser system. J. Frankl. Inst. **354**, 8117–8133 (2017)
32. Zhao, Z., He, X., Ren, Z., Wen, G.: Boundary adaptive robust control of a flexible riser system with input nonlinearities. IEEE Trans. Syst. Man Cybern. Syst. (2018). https://doi.org/10.1109/TSMC.2018.2882734
33. Zhao, Z., He, X., Member, S., Ren, Z., Wen, G.: Output feedback stabilization for an axially moving system. IEEE Trans. Syst. Man, Cybern. Syst. (2018). https://doi.org/10.1109/TSMC.2018.2882822
34. Liu, Y., Zhang, K., Zhang, W.Z., Meng, X.Y.: Wave-based vibration control of large cable net structures. Wave Motion. **77**, 139–155 (2018)
35. Guo, B., Shao, Z.: Stabilization of an abstract second order system with application to wave equations under non-collocated control and observations. Syst. Control Lett. **58**, 334–341 (2009)
36. Tan, C.A., Ying, S.: Active wave control of the axially moving string: theory and experiment. J. Sound Vib. **236**, 861–880 (2000)
37. Zingoni, A.: An efficient computational scheme for the vibration analysis of high tension cable nets. J. Sound Vib. **189**, 55–75 (1996)
38. Elmore, W.C., Heald, M.a, Roelofs, L.: Physics of Waves. McGraw-Hill, Cambridge (1969)
39. Xu, X., Zuo, S., Zhang, K., Hu, G.: Wave-based transfer matrix method for dynamic response of large net structures. J. Sound Vib. **433**, 265–286 (2018)
40. Doyle, J.F.: Wave Propagation in Structures. Springer, Berlin (1989)
41. Kovacic, I., Brennan, M.J.: On the use of two classical series expansion methods to determine the vibration of harmonically excited pure cubic oscillators. Phys. Lett. A. **372**, 4028–4032 (2008)
42. Lax, P.D.: Weak solutions of nonlinear hyperbolic equations and their numerical computation. Commun. Pure Appl. Math. **7**, 159–193 (2010)
43. Wang, L., Dongxu, L., Jianping, J.: General mesh configuration design approach for large cable-network antenna reflectors. J. Struct. Eng. **140**, 04013051 (2014)
44. Liu, W., Lia, D.X., Jiang, J.P.: Mesh topological form design and geometrical configuration generation for cable-network antenna reflector structures. Struct. Eng. Mech. **45**, 407–418 (2013)
45. Schek, H.J.: The force density method for form finding and computation of general networks. Comput. Methods Appl. Mech. Eng. **3**, 115–134 (1974)